Optical parametric oscillation in soliton-induced waveguides

Song Lan

Department of Electrical Engineering, Princeton University, Princeton, New Jersey 08544

J. A. Giordmaine

Department of Electrical Engineering, Princeton University, Princeton, New Jersey 08544, and NEC Research Institute, Princeton, New Jersey 08540

Mordechai Segev

Department of Physics, Technion–Israel Institute of Technology, Haifa 32000, Israel, and Department of Electrical Engineering, Princeton University, Princeton, New Jersey 08544

Daniel Rytz

Forschungsinstitut für Mineralische und Metallische Werkstoffe-Edelstein/Edelmetalle-GmbH, Struthstrasse 2, D-55743 Idar Oberstein, Germany

Received December 4, 2001

We demonstrate experimentally an optical parametric oscillator constructed in a waveguide induced by a photorefractive spatial soliton and show that the pumping threshold is reduced considerably. © 2002 Optical Society of America

OCIS codes: 190.5530, 190.2620, 190.5330, 230.7370, 260.1180.

Photorefractive spatial solitons[1] and the waveguides that they induce[2] offer potential applications, some of which are truly unique[3]: reconfigurable near-field interconnects, three-dimensional optical circuitry,[4,5] directional coupling,[6,7] beam steering,[8] and nonlinear frequency conversion.[9,10] The properties that make photorefractive soliton-induced waveguides so interesting are dimensionality, wavelength sensitivity, and fixability. Dimensionality means that the solitons self-trap in (2 + 1) dimensions and the induced waveguides are two dimensional (2D),[11] which facilitates 2D directional couplers[6] and three-dimensional optical circuitry.[4,5] Wavelength sensitivity results from the fact that photorefractivity is driven by charge carriers that are photoexcited from impurities, so the photoexcitation cross section varies with wavelength. One can generate a photorefractive soliton at a highly photosensitive wavelength and guide a probe beam in the soliton's induced waveguide at a nonsensitive wavelength. Fixability is the ability to impress the soliton-induced waveguides into the crystalline lattice and create fixed waveguides. Such waveguides can be written, erased, and rewritten with a different profile or in a different direction by virtue of the interplay of temperature, electric field, and the hysteresis curve.[4,5,12]

The most promising application of waveguides induced by photorefractive solitons is nonlinear frequency conversion. The conversion efficiency in $\chi^{(2)}$ processes is proportional to the intensity of the pump beam, so it is desirable to work with very narrow beams. One easy way to achieve narrow beams is to launch a focused pump beam. However, in a bulk crystal, the more focused a beam is, the faster it diffracts, and diffraction limits the frequency-conversion efficiency because as the interacting beams diffract (1) their intensities decrease and (2) the phase-matching condition cannot be satisfied across the entire cross section of beams. Therefore, using waveguides for frequency conversion can greatly improve conversion efficiency. But thus far it has been difficult to fabricate waveguides from most materials that allow for phase matching, and 2D waveguides are especially difficult to make. However, 2D photorefractive solitons induce 2D waveguides, and almost all photorefractives are highly efficient in $\chi^{(2)}$ frequency conversion. In waveguides, phase matching should take place among the propagation constants of the guided modes and is typically obtained through birefringence or periodic poling. In a fabricated waveguide, however, the structure is fixed, so tuning techniques rely on varying the temperature[13] or on lateral translation in structures with several periods of poling that are parallel to one another.[14] But waveguides induced by photorefractive solitons offer much flexibility because their waveguide structures and propagation axes (with respect to the crystalline axes) can be modified at will and in real time.[10] Working with photorefractive solitons, one can achieve wavelength tunability while avoiding diffraction by simply rotating the crystal and launching a soliton in the new direction. One can also fine tune the frequency-conversion process by changing the propagation constants of the guided modes through varying the intensity ratio and external voltage, allowing tuning with no mechanical movements.

In our earlier work we have demonstrated second-harmonic generation in waveguides induced by photorefractive solitons and have shown that the conversion efficiency can be considerably increased[9] and high tunability can be obtained by rotation of the crystal.[10] Another important system for nonlinear frequency conversion is the optical parametric oscillator (OPO). In an OPO the threshold pump power

0146-9592/02/090737-03$15.00/0

is dependent on the signal gain per pass through the crystal. To lower the threshold, one has to increase the signal gain per pass. A waveguide that confines the pump beam as well as the signal and idler in a small area is one very effective way to do this. Consider a Gaussian beam at the pump frequency launched into a nonlinear crystal and assume that phase matching is satisfied at the waist, located at the input surface. The threshold pump power is proportional to $[z_0 \arctan^2(L/z_0) + \ln^2(1 + L^2/z_0{}^2)/4]^{-1}$, where z_0 is the Rayleigh (diffraction) length of the beam and L is the crystal length.[15] For a given L, there exists an optimum beam size for minimum threshold pump power, when $z_0 = L/2.84$. However, if a waveguide is used to keep all beams at the same widths throughout propagation in the crystal, the threshold is simply proportional to z_0/L^2, which continues to decrease as we focus the beam more. The minimum threshold is determined by the smallest size of the waveguide that can be made. To estimate the improvement, consider a focused Gaussian beam with a minimum beam waist of 21 μm and a 15-mm-long crystal. An OPO constructed in a waveguide has a threshold pump power 60% lower than that of an OPO with the same beam waist in bulk. Therefore, in a waveguide OPO the signal gain per pass can be considerably improved, and the threshold pump power can be substantially lowered for the same cavity loss. Here we demonstrate an OPO in a waveguide induced by a photorefractive soliton and show that the OPO threshold is significantly lowered.

Our setup is shown in Fig. 1. We construct a doubly resonant oscillator in which the oscillation occurs at both the signal and the idler wavelengths. Compared with a singly resonant oscillator in which only the signal beam resonates, this oscillator requires lower threshold pump power and can be pumped by an ordinary cw laser source. The oscillator consists of two concave mirrors with 2.5-cm radius and a nonlinear crystal. The mirrors are coated to yield 98% transmission for the pump light and high reflectivities (99.8–99.9%) for the signal and the idler beams. A 488-nm argon laser acts as the pump beam and also forms the soliton via photorefractivity. An optical isolator is used to prevent laser instability caused by reflection from the mirrors and the crystal. The beam is adjusted to match the fundamental mode of the cavity, and the minimum beam waist is located at the input surface of the crystal. A chopper forms 150-μs pump pulses with a repetition rate of 67 Hz. For pulses of this duration, the parametric process is essentially cw pumped, and the peak gain is determined by the peak power of the pump pulses. However, the pulse duration is much shorter than the response time of the photorefractivity, so the structure of the soliton is dependent on only the average power of the pump beam. Therefore, we control the parametric process with the pump power and the on–off ratio of the chopper independently. The nonlinear crystal is a photorefractive 5 mm $\times$ 15.8 mm $\times$ 5 mm ($a \times b \times c$) $KNbO_3$ crystal. All beams propagate along the b axis, and the external voltage is applied along the c axis. The pump is polarized along the c axis, whereas the signal and the idler are both polarized along the a axis. We use temperature control to tune the output wavelengths via phase matching. The crystal is also illuminated uniformly by a white-light beam as the necessary background for the photorefractive screening nonlinearity.[11]

First we operate the OPO without soliton-induced waveguiding. Starting with a pump power of 200 mW, we obtain oscillation by fine alignment of the mirrors. Figure 2 shows the cross sections of the pump and the signal beams. The 488-nm beam is focused at the input surface of the crystal with a FWHM of 21 μm, as shown in Fig. 2a. The minimum waist of the signal beam is also located at the input surface of the crystal with a FWHM of 28 μm (Fig. 2b). At the output surface the pump beam diffracts to 54 μm (Fig. 2c), and the signal beam size is 69 μm (Fig. 2d). The signal and the idler wavelengths are 830 and 1186 nm, respectively, at a temperature of 40 °C, as shown in Fig. 3a. We also measure the output signal peak power as a function of pump power (see the squares in Fig. 3b). The threshold pump power is measured to be 84 mW.

Next, we investigate the operation of the OPO with the soliton. Comparing the mode structure of the resonator with the soliton and without the soliton, we find that to use the same Gaussian beam waist diameter

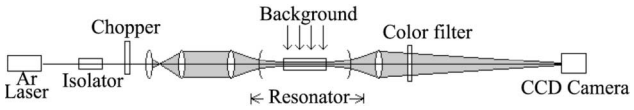

Fig. 1. Experimental setup.

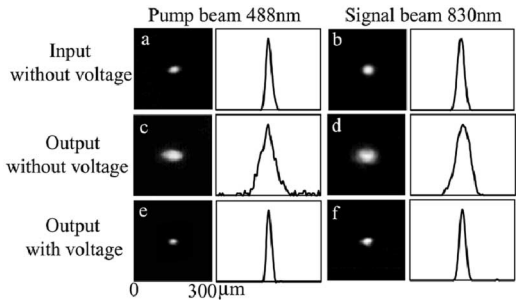

Fig. 2. Beam cross-section profiles at crystal input and output surfaces. a, Pump beam at the input without voltage; b, signal beam at the input without voltage; c, pump beam at the output without voltage; d, signal beam at the output without voltage; e, pump beam at the output with voltage, which is the soliton output; f, signal beam at the output with voltage, guided by the soliton.

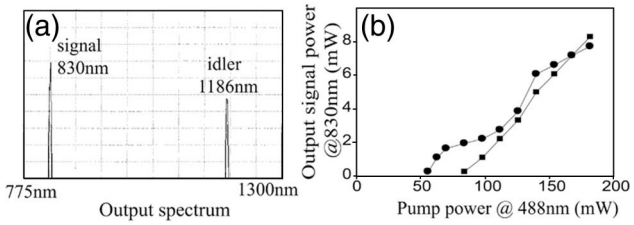

Fig. 3. OPO output results: a, output spectrum; b, output signal power versus input pump power.

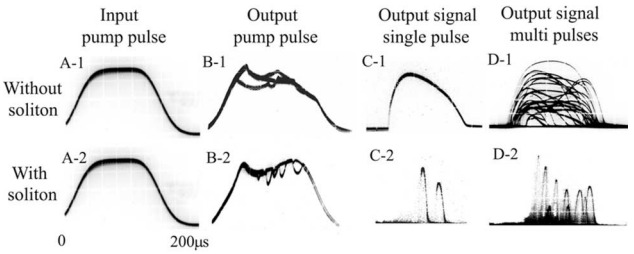

Fig. 4. Pulse shapes of the pump beam and the output signal.

we need to increase the cavity length by a distance of L/n, in which n is the crystal refractive index. To do this in our setup, we move the back mirror 7.09 mm away from the crystal. We turn the external field on and generate the soliton. We then obtain oscillation, optimize the voltage and the intensity ratio, and find the maximum output signal power. At the optimum operation point, the intensity ratio (the average pump intensity at the center of the beam over the background intensity) is 24, and the external voltage is 2.82 kV. The beam profiles are shown in Fig. 2. The soliton at the output is shown in Fig. 2e, and the guided signal beam in Fig. 2f. The widths of the output beams are identical to those in the input surface. Comparing Figs. 2f and 2d, we can see that the OPO operates with guidance of the induced waveguide. The output signal power as a function of pump power is shown in Fig. 3b. The OPO with soliton-induced waveguiding operates with a pump threshold power of 56 mW, which is 33% lower than that of the OPO without the soliton.

We note that at the highest pump power levels in our experiment the output signal is slightly weaker than without the soliton. This is because our resonator is doubly resonant. When the signal and the idler beams propagate in the reverse direction, energy is transferred back to the pumping wavelength. Consequently, when we launch the soliton and form the waveguide, the reverse process is also enhanced. The improvement in the counterproductive reverse process limits the efficiency of the oscillator, but this can be readily resolved by use of a singly resonant oscillator or by use of a ring oscillator. Another problem caused by the doubly resonant nature of our OPO is its instability. The instability of doubly resonant OPOs is an extensively studied issue, and it becomes more serious when we use the soliton-induced waveguide. This instability can be observed in the pulse shapes of the pump and the output signal. The insets A-1 and A-2 in Fig. 4 show the input pump pulses entering the resonator. The pump pulse leaving the resonator (B-1, Fig. 4) shows the energy transfer to the signal and the idler. In Fig. 4, C-1 and D-1 show the output signal pulses, taken with one and with multiple pump pulses, respectively. One can see large amplitude fluctuations. The reason for these fluctuations is that in doubly resonant OPOs the signal and the idler frequencies not only have to be phase matched but also have to coincide with the resonant frequencies of the resonator. The oscillation is very sensitive to the frequency shift of the pump beam and the length variation of the resonator.[16] When we apply voltage and generate the soliton, the pump beam after the resonator, B-2, is shown in Fig. 4. Single-pulse and multipulse pictures of the output signal are shown by C-2 and D-2, respectively, in Fig. 4. It is apparent that, in addition to the amplitude fluctuations, the output signal appears as shorter pulses, with an average pulse width of 20 μs. This is consistent with the additional constraint that the signal and idler modes are strongly soliton guided, making the oscillation more sensitive to small change in the resonator. The stability of our soliton-induced OPO can be greatly improved by use of a singly resonant OPO.

In conclusion, we have demonstrated an optical parametric oscillator in a waveguide induced by a photorefractive soliton and have shown that the threshold pump power is significantly reduced. This technique should work much better with singly resonant OPOs, and it can substantially reduce the threshold pump power when very narrow solitons are employed. For example, if we use a soliton beam with a beam waist of 8 μm and a 15-mm crystal, we can reduce the threshold pump to only 3.5% of that for an OPO in the same nonlinear medium, using the same mirrors but without the soliton.

This work was supported by the U.S. Army Research Office, the National Science Foundation, and the Israeli Science Ministry. M. Segev's e-mail address is msegev@tx.technion.ac.il.

References

1. M. Segev, B. Crosignani, A. Yariv, and B. Fischer, Phys. Rev. Lett. **68,** 923 (1992).
2. M. Shih, Z. Chen, M. Mitchell, M. Segev, H. Lee, R. S. Feigelson, and J. P. Wilde, J. Opt. Soc. Am. B **14,** 3091 (1997).
3. M. Segev, M. Shih, and G. Valley, J. Opt. Soc. Am. B **13,** 706 (1996).
4. M. Klotz, H. Meng, G. J. Salamo, M. Segev, and S. R. Montgomery, Opt. Lett. **24,** 77 (1999).
5. A. Guo, M. Henry, G. Salamo, and M. Segev, Opt. Lett. **26,** 1274 (2001).
6. S. Lan, E. DelRe, Z. Chen, M. Shih, and M. Segev, Opt. Lett. **24,** 475 (1999).
7. J. Petter and C. Denz, Opt. Commun. **188,** 55 (2001).
8. E. DelRe, M. Tamburrini, and A. J. Agranat, Opt. Lett. **25,** 963 (2000).
9. S. Lan, M. Shih, G. Mizell, J. A. Giordmaine, Z. Chen, C. Anastassiou, J. Martin, and M. Segev, Opt. Lett. **24,** 1145 (1999).
10. S. Lan, C. Anastassiou, M. Shih, J. A. Giordmaine, G. Mizell, and M. Segev, Appl. Phys. Lett. **77,** 2101 (2000).
11. M. Shih, M. Segev, and G. Salamo, Opt. Lett. **21,** 931 (1996).
12. E. DelRe, M. Tamburrini, M. Segev, R. D. Pergola, and A. J. Agranat, Phys. Rev. Lett. **84,** 1954 (1999).
13. M. M. Fejer, G. A. Magel, D. H. Jundt, and R. L. Byer, IEEE J. Quantum Electron. **28,** 2631 (1992).
14. L. E. Myers, R. C. Eckardt, M. M. Fejer, R. L. Byer, and W. R. Bosenberg, Opt. Lett. **21,** 591 (1996).
15. G. D. Boyd and D. A. Kleinman, J. Appl. Phys. **39,** 3597 (1968).
16. R. G. Smith, IEEE J. Quantum Electron. **9,** 530 (1973).